Research Article

Yunfeng Ma, Qiyao Liu*, Yushan Bian, Lei Feng, Di Zhao, Shuai Wang, Huijie Zhao, Kunyu Gao, and Zhengqing Xu

Analysis of transport path and source distribution of winter air pollution in Shenyang

https://doi.org/10.1515/geo-2020-0292
received May 07, 2021; accepted August 11, 2021

Abstract: Air pollution is one of the most serious environmental problems faced by mankind. It is regional and highly complex, and it is more prominent in China. With the development of air quality management in China, the research on cross-regional transmission of air pollutants is particularly important. This paper reports on pollution characteristics, transport path, and distribution of pollution sources of major contaminants in Shenyang. For this purpose, pollution-monitoring data were gathered from November 2017 to March 2018. Data were analyzed using the HYSPLIT back trajectory model, the potential source contribution function (PSCF), and the concentration weighted trajectory (CWT) model. Results indicated that $PM_{2.5}$ was the main pollutant in Shenyang during the study period. Air pollution was mainly affected by coal combustion, traffic emissions, and long-distance transmission. Among the 11 monitoring points, the pollution of Shenliaoxilu was relatively serious. Mongolia, eastern Inner Mongolia, northwestern Jilin, and most of Liaoning were the main potential sources of $PM_{2.5}$ in Shenyang during the winter.

Keywords: pollution sources, pollution characteristics, HYSPLIT, TrajStat, PSCF, CWT

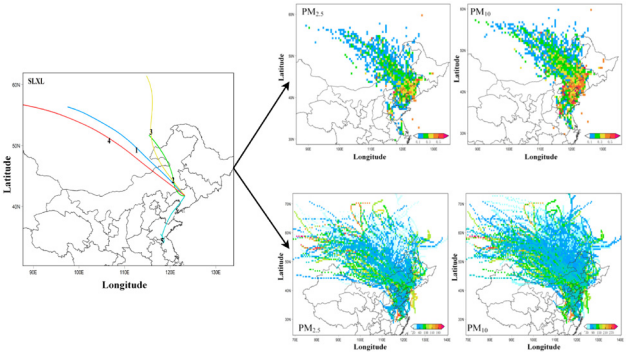

Graphical abstract

1 Introduction

Air pollution has become a global challenge; it has harmful effects on health, ecology, and people's lives [1]. By analyzing the results of concentration weighted trajectory (CWT) and potential source contribution function (PSCF), Dimitriou (2015) determined the potential sources of PM in Valencia, Spain [2]. Gibergans-Baguena et al. (2020) proposed a new air quality index (AQI) based on component data analysis in Barcelona [3]. In Republic of North Macedonia, Angelevska et al. (2021) designed a guide to urban air quality, which is based on road traffic management measures [1].

In recent years, the industrialization in China has significantly grown. As a result, haze pollution has also increased becoming a serious problem, for example, causing a decrease in visibility which has caught the attention of the ordinary people, experts, and scholars. Chinese State Council issued strict new air-pollution laws in 2014 [4]. In 2017, 70.7% of Chinese 338 prefectures and above cities failed to meet the National Ambient Air Quality Standards of China (NAAQS) [5]. In January 2018, the monthly average maximum concentration of $PM_{2.5}$, PM_{10}, SO_2, and NO_2 in 74 major cities in China were 141, 191, 69, and 76 $\mu g/m^3$, respectively [6]. Besides, per capital $PM_{2.5}$ in Chinese major cities was 61 $\mu g/m^3$, which was three times that for the global average value [7]. Based on the ground monitoring data of $PM_{2.5}$

* **Corresponding author: Qiyao Liu,** College of Energy and Environment, Shenyang Aerospace University, Shenyang 110136, China, e-mail: 2078758@qq.com
Yunfeng Ma, Lei Feng, Huijie Zhao: College of Energy and Environment, Shenyang Aerospace University, Shenyang 110136, China
Yushan Bian: 3Clear Technology Co. Ltd., Beijing 100000, China
Di Zhao: Shenyang Academy of Environmental Sciences, Shenyang 110167, China; Liaoning Provincial Key Laboratory of Atmospheric Environmental Pollution Prevention and Control, Shenyang 110167, China
Shuai Wang: Shenyang Ecological Environment Monitoring Center of Liaoning Province, Shenyang 110169, China
Kunyu Gao: Affairs Service Center of Ecological Environment of Liaoning Province, Shenyang 110161, China
Zhengqing Xu: Chongqing Liangjiang Satellite Mobile Communication Co., Ltd. Chengdu Branch, Chengdu 610065, China

concentration in 366 cities in China in 2016, Chen et al. established a more sustainable cross-regional joint management strategy [8]. The air pollution during winter season in northern China becomes particularly severe. In this area, the air pollution is mainly caused by the bad weather conditions, high coal consumption, and urban traffic emissions [9–11].

Shenyang is located in the northeast of China and central Liaoning Province. It presents a typical semi-humid continental climate. Its economic activity is dominated by industry, and coal has been used as the chief energy source, and the annual consumption is 35 million tons [12]. As the only megacity in the Northeast, Shenyang displays an urbanization rate of 81% and air pollution is becoming worse with time [13]. From 2010 to 2012, Shenyang presented average monthly visibilities of 19.0 ± 4.3 and 17.1 ± 4.3 km for the months of March and September, respectively. These values were relatively high. Corresponding data for January were about 11.0 ± 4.7 km, which was relatively low [14]. In November 2015, serious air pollution appeared in northeastern China, where the maximum hourly $PM_{2.5}$ concentration in Shenyang exceeded 1,000 μg/m^3 [15]. Miao et al. (2018) studied the influence of weather patterns on aerosol transport and the planetary boundary layer in Shenyang during December 1–3, 2016. It was found that the atmospheric aerosol pollution in Shenyang had relation to local atmospheric emissions and atmospheric aerosol transboundary migration. According to the data, the aerosol released from Beijing-Tianjin-Hebei region may be brought to Shenyang under the influence of westerly wind and southwest wind [16]. Authors concluded that there is an imperative requirement for controlling air pollution in this region. Meanwhile, since the diffusion and transport of air pollutants can pose a great challenge to pollution control, the identification and quantification of pollution sources are key to controlling pollutant concentrations [17]. Pollutants transported across regions contribute significantly to changes in air quality. Even if there are studies on the characteristics of air pollutants in Shenyang, most of the existing studies focus on the analysis of short-term pollution events [18–20].

In this work, hourly $PM_{2.5}$, PM_{10}, SO_2, NO_2, O_3, and CO concentrations were obtained from the national air quality-monitoring network in 11 different stations in Shenyang. This information was combined with meteorological data so as to analyze the spatial and temporal distribution characteristics of air pollutants in Shenyang. The back trajectory model, PSCF, and CWT were also used to study the transport path and source distribution of the pollutants. Shenyang contaminants concentrations were compared with those found in other major cities in China. The results of the study are conducive to comprehend the main characteristics of winter air pollution in Shenyang. In addition, it is possible to identify potential sources of environmental pollutants. This will assist decision-makers in designing effective strategies for air pollution control. The results can provide guidance for the future control strategy and policy-making in Northeast China.

The rest of the paper is organized as follows: Section 2 introduces the source of data and research methods. Next, in Section 3 we report the experiments in detail and discuss the experimental results. Finally, a brief conclusion is drawn in Section 4.

2 Materials and methods

2.1 Data collection

For this research, 11 monitoring points of the National Air Quality-Monitoring Network were selected. The monitoring data from the eleven monitoring points were obtained from the Ministry of Ecology and Environment of China (http://www.mee.gov.cn/). The monitoring methods for $PM_{2.5}$ and PM_{10} are β-ray absorption method (dynamic heating DHS) and light scattering method (optical turbidity); Pulse ultraviolet fluorescence method is used for SO_2 monitoring; NO_2 monitoring uses chemiluminescence method; CO monitoring method is gas filter correlation infrared Absorptiometry; O_3 is monitored by ultraviolet photometry. During the monitoring, calibration using NO, CO, and SO_2 standard gases produced by the National Institute of Metrology, and the Thermo 49 i-PS UV photometer O_3 calibrator was used to calibrate the O_3 analyzer. Each instrument needs to be calibrated once every 7 days and the sampling pipeline is cleaned at least once a month, so as to ensure the accuracy and effectiveness of the monitoring data. Six conventional pollutants at hourly concentrations at the 11 stations in Shenyang during the central heating period (November 1st, 2017 to March 31st, 2018) were analyzed. The 11 air quality-monitoring points were: Donglinglu (DLL; 41.841°N, 123.590°E), Hunnandonglu (HNDL; 41.741°N, 123.505°E), Jingshenjie (JSJ; 41.923°N, 123.378°E), Lingdongjie (LDJ; 41.847°N, 123.426°E), Senlinlu (SLL; 41.934°N, 123.684°E), Shenliaoxilu (SLXL; 41.735°N, 123.244°E), Taiyuanjie (TYJ; 41.797°N, 123.402°E), Wenhualu (WHL; 41.765°N, 123.411°E), Xiaoheyan (XHY; 41.787°N, 123.468°E), Xinxiujie (XXJ; 41.699°N, 123.423°E), and Yunonglu (YNL; 41.909°N,

123.595°E), respectively. The locations of Shenyang in China and 11 monitoring points are shown in Figure 1. SLL is located in Qipanshan, and it was used as the background level since it does not contain a pollution source. Other selected points were close to different emission sources, including transportation and industry.

In this study, weather data (wind speed, wind direction, and temperature) were collected every 3 h from the National Climate Data Center in Shenyang. Since data were scarce, the information obtained in one station was analyzed to represent the general weather. Even when no exact information for every site of analysis existed, this approach may provide a reference to understand the correlation between weather and atmospheric pollution in Shenyang. In the study period, the average temperature was −5.17°C. The dominant wind is from the north and the mean wind speed is 2.18 m/s. A probability of wind speed less than 2 m/s exceeds 50 units. At this speed, pollutants' concentration showed a peak value; in addition, the lowest visibility was observed.

In the present research, the 8-hourly, daily mean, and monthly average concentrations of six conventional pollutants were used as the average values of the data recorded by the hour. Twenty-four hour pollutant concentration was calculated only when effective data for more than 20 h were available on a given day. The average 8 h O_3 concentration was calculated using valid data from at least 6 h. In addition, monthly average was calculated using the average of the hourly data for the whole month. Unless otherwise stated, the pollutant concentration reported for each monitoring point in Shenyang represents the data average for that site.

2.2 Model

For purpose of determining the potential impact of cross-region wind transport on air pollutants' concentrations in Shenyang, HYSPLIT4 (the Hybrid Single-Particle Lagrangian Integrated Trajectory model version 4 developed by NOAA) was used to calculate the back trajectories of the air mass during this survey [21,22]. The HYSPLIT model is a complete system that calculates simple air mass trajectories through complex diffusion and deposition simulations, and it is able to calculate the source and transport of air blocks to a particular research location. Model calculation uses meteorological data with one degree and one degree spatial resolution of GDAS [22]. A 72 h backward trajectory was calculated from November 1st, 2017 to March 31st, 2018. For this, a height of 500 m for two sites (SLL and SLXL) and four different times (local time 00:00, 06:00, 12:00, and 18:00 h) were considered every day. The calculated trajectory was processed using a cluster analysis method.

The PSCF and CWT methods were used to determine the possible source areas and their contribution to the mass concentration of air pollutants. Analysis was on the basis of the backward trajectory model. In addition, TrajStat was also applied [23]. The probability map of the area around the study location during the research is

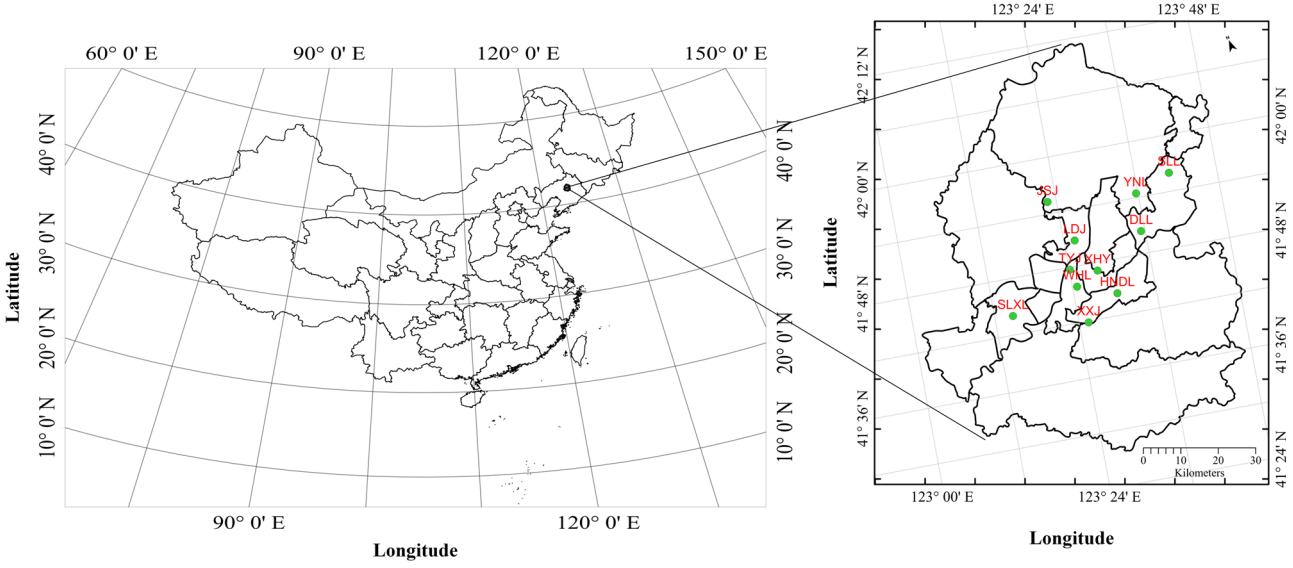

Figure 1: Location (shadow) and monitoring points (solid circles) in Shenyang, China, used in the present research.

often generated using the PSCF method [20,24]. This is a method that locates the potential source affecting the air quality of the receptor site on the basis of the residence time and air mass distribution in a particular area [25]. When the concentration is higher than the standard value determined by the user, the obtained PSCF value can be regarded as a conditional probability associated with the trajectory of the air mass having the PSCF value reaching the research site through the mesh unit. A greater PSCF value indicates a greater probability. In our current research, the $PM_{2.5}$ limit was set to 75 μg/m^3 and the PM_{10} limit was set to 100 μg/m^3, according to the NAAQS GradeIIlimited value. The CWT method can assess the contribution of possible pollution sources to the contaminant concentration at a certain study site with result of the air mass trajectory weighted concentration [26–28]. A higher CWT value indicates a higher potential contribution to a heavy contamination of the monitor site. In this work, PSCF and CWT methods took into account the concentrations of $PM_{2.5}$ and PM_{10} in SLL and SLXL, respectively. The specific research methods are shown in Figure 2.

3 Results and discussion

3.1 Time distribution of pollutants

The time series of CO, O_3, SO_2, and NO_2 particulate matter with aerodynamic diameters of <2.5 μm ($PM_{2.5}$) and <10 μm (PM_{10}) concentrations at the eleven monitoring stations were selected for this study. As shown in Figure 3, it was found that for the periods December 29–31, 2017, February 25–28, 2018, and March 23–26, 2018, concentrations of CO, O_3, SO_2, NO_2, $PM_{2.5}$, and PM_{10} significantly increased. This resulted in three significant pollution events. These three periods displayed average hourly AQI greater than 150 at every monitoring station to the exclusion of SLL, which indicated severe atmospheric pollution. The mean data corresponding to the three high pollution incidents indicated that average daily concentrations (and IAQI) of CO, O_3, SO_2, NO_2, $PM_{2.5}$, and PM_{10} in the city were 1.797 mg/m^3(45), 60(30), 48(48), 57(71), 119(156), and 162(106) μg/m^3, respectively. In addition, the hourly peak concentrations were 3.845 mg/m^3(96), 214(149), 105(78), 105(113), 228(311), and 302(176) μg/m^3, respectively. Among the eleven monitoring points, SLXL displayed the peaked $PM_{2.5}$ and PM_{10} concentrations, with average daily peaks of 174 and 228 μg/m^3, respectively. This may be because Tiexi District is developed in industry with many factories. This is in line with the findings of Tian et al. [29]. These values were twice the NAAQS Grade II limited value. Even at the background point (labeled as SLL), the 24 h $PM_{2.5}$ concentrations exceeded 75 μg/m^3, and the peak concentration reached 129 μg/m^3, indicating the possibility of regional pollution and pollutant transport. Figure 3 shows that these peaks occurred at a low wind speed (<1 m/s) and southwest winds. At the same time, strong winds (>5 m/s) from the southwest were associated with a cleaner air. The southeast wind or the east wind may transport polluted air from other parts of the Liaoning Province. In general, low speed winds from the south and east may be related to the accumulation of pollutants, which may be emitted locally or transported from other regions.

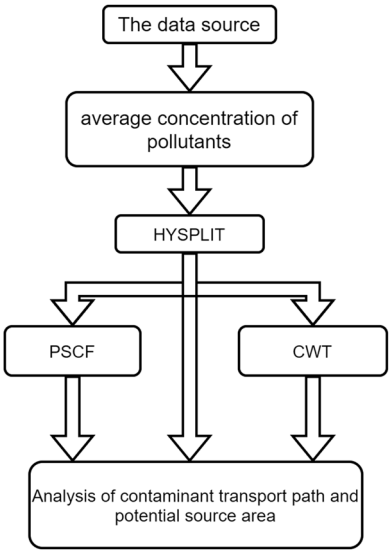

Figure 2: The flowchart of main research methods.

To further determine the characteristics of PM pollution, the $PM_{2.5}/PM_{10}$ was calculated (Figure 3). As a part of PM_{10}, $PM_{2.5}$ plays an extremely significant role in the ratio analysis of 0–10 μm particle size distribution. Therefore, the clear ratio relationship between $PM_{2.5}$ and PM_{10} can be used as a reference for pollution source analysis and prevention. The ensemble average $PM_{2.5}/PM_{10}$ value for Shenyang was 0.73, which was slightly higher than the mean level for other cities across the country [30]. As shown in Figure 3, the peak pollutant concentration mostly corresponds to a relatively greater $PM_{2.5}/PM_{10}$ value. At the severe contamination days, this ratio was mostly >0.7. According to relevant literature reports, $PM_{2.5}$ has a greater impact on air pollution and extinction than PM_{10} [31,32]. However, in order to further study the interaction between PM and air pollution, it is essential to conduct much deeper research on the chemical composition and atmospheric visibility of PM.

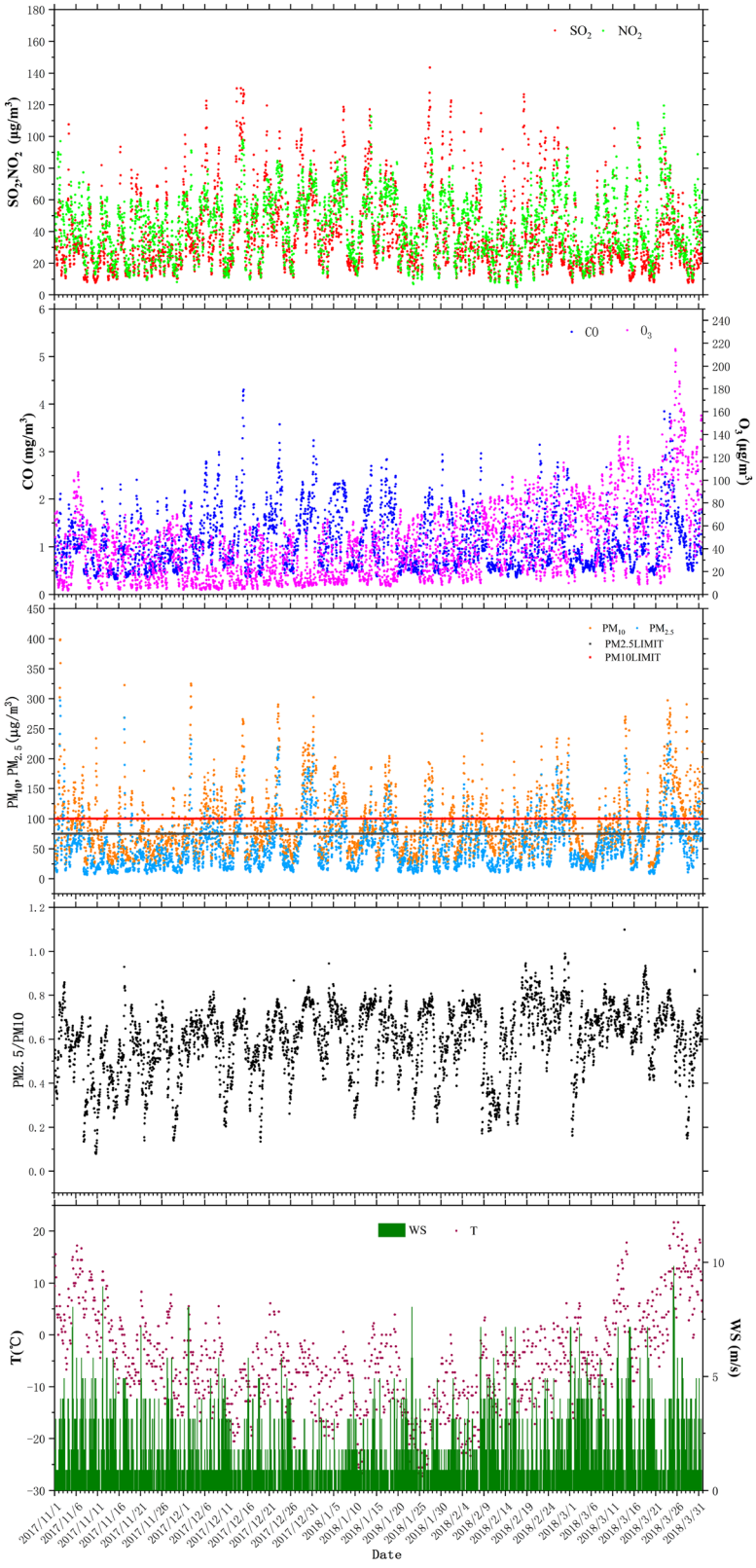

Figure 3: Concentrations of CO, O_3, SO_2, NO_2, $PM_{2.5}$, and PM_{10}, T and WS (wind speed) during the research period.

3.2 Concentration patterns

From November 1st, 2017 to March 31st, 2018, the hourly mean concentrations of $PM_{2.5}$, PM_{10}, SO_2, NO_2, 8 h O_3, and CO in Shenyang were 55, 88, 37, 42, and 42 μg/m^3, and 1.114 mg/m^3, respectively. The average environmental pollutant concentrations at the eleven points studied in this research are shown in Table 1. The pollution level of SLXL was generally the highest, followed by HNDL. In addition, the air in SLL was the cleanest. The 24 h mean concentrations of $PM_{2.5}$, PM_{10}, and CO in SLXL were the highest (183 and 243 μg/m^3 and 3.167 mg/m^3, respectively). At the same time, peak concentrations of SO_2 and NO_2 appeared in TYJ and LDJ, and O_3 concentration peak appeared in JSJ and SLXL. $PM_{2.5}$ is the major pollutant at each research site, which proves that high levels of $PM_{2.5}$ were the primary cause of air pollution in Shenyang during the study period.

The $PM_{2.5}$, PM_{10}, and NO_2 24 h mean values in Shenyang were compared with the NAAQS GradeIIlimited values. The concentrations of SO_2, O_3, CO, and NO_2 were all below the NAAQS GradeIIlimited values, whereas the concentrations of $PM_{2.5}$ and PM_{10} clearly exceeded mandatory standards. According to the data, average $PM_{2.5}$ reached the NAAQS standard during 113 days, which represents a 74.8% of the total number of days (151) when simultaneous measurements at the eleven monitoring points were performed. The fractions of $PM_{2.5}$ exceeding the standard day values in the eleven monitoring points were between 9.93% (SSL) and 30.46% (HNDL), and the fraction of PM_{10} exceeding the standard day values was between 2.64% (SLL) and 14.56% (SLXL). $PM_{2.5}$ concentrations exceeded standard values in a higher ratio as compared to other pollutants. The study found that $PM_{2.5}$ was the major contamination in Shenyang with poor atmospheric visibility and serious pollution.

Daily variation of the studied pollutants was estimated based on the hourly measured data. We needed to use this information to identify potential sources of emissions. Figure 4 shows the monthly average daily variation of $PM_{2.5}$, SO_2, NO_2, O_3, and CO in Shenyang. According to Figure 4, the highest concentration of $PM_{2.5}$ and CO appeared in December and ranked second in February. In addition, the concentrations of SO_2 and NO_2 were sighted to be higher in December and January. In December, the hourly mean concentrations of $PM_{2.5}$ and CO were >60 μg/m^3 and 1.155 mg/m^3, respectively. By relating these data to changes in wind speed (Figure 3), it was observed that at higher frequencies of the low wind speed in December, a higher pollution level was likely to occur. And, due to the low wind speed, pollutants are not easy to spread. Therefore, it can be concluded that wind speed is negatively correlated with $PM_{2.5}$ concentration.

SO_2 displayed a similar daily variation graph during the five months. The same was observed for NO_2, and CO. In every month, NO_2 and CO show two peaks at about 9:00 and 20:00 h, which corresponded to peak hours. Thus, it is likely that this pollution proceeds from vehicle emissions [33]. Also, a concentration increase was observed after 21:00 h, which was probably due to an increment in the boundary layer. O_3 reached its peak value at 14:00 h, while NO_2 concentration decreased at this time, indicating that NO_2 is negatively correlated with O_3 concentration due to photochemical reaction [34]. This is similar to previous research [29,35]. It was also observed that every month, SO_2 concentration reached a peak between 9:00 and 11:00 h. An increasing trend started again after 16:00 h. This was probably owing to changes in meteorological conditions such as differences in boundary layer height. Since the study was carried

Table 1: Hourly average concentration of pollutants and AQI at 11 sites during the study period (Units: CO in mg/m^3; other pollutants' concentrations are given in μg/m^3)

Site	Description	AQI	$PM_{2.5}$	PM_{10}	SO_2	NO_2	O_3	CO
DLL	Donglinglu	74	54	84	34	35	45	1.130
HNDL	Hunnandonglu	84	62	95	36	43	40	1.177
JSJ	Jingshenjie	76	56	84	37	43	47	1.111
LDJ	Lingdongjie	71	52	91	44	51	43	1.120
SLL	Senlinlu	63	45	67	23	27	57	1.011
SLXL	Shenliaoxilu	86	64	103	37	40	47	1.117
TYJ	Taiyuanjie	79	58	88	53	51	33	1.204
WHL	Wenhualu	79	58	95	42	49	35	1.101
XHY	Xiaoheyan	75	55	91	43	51	37	1.191
XXJ	Xinxiujie	79	58	95	34	46	39	1.125
YNL	Yunonglu	69	50	73	30	37	47	0.982

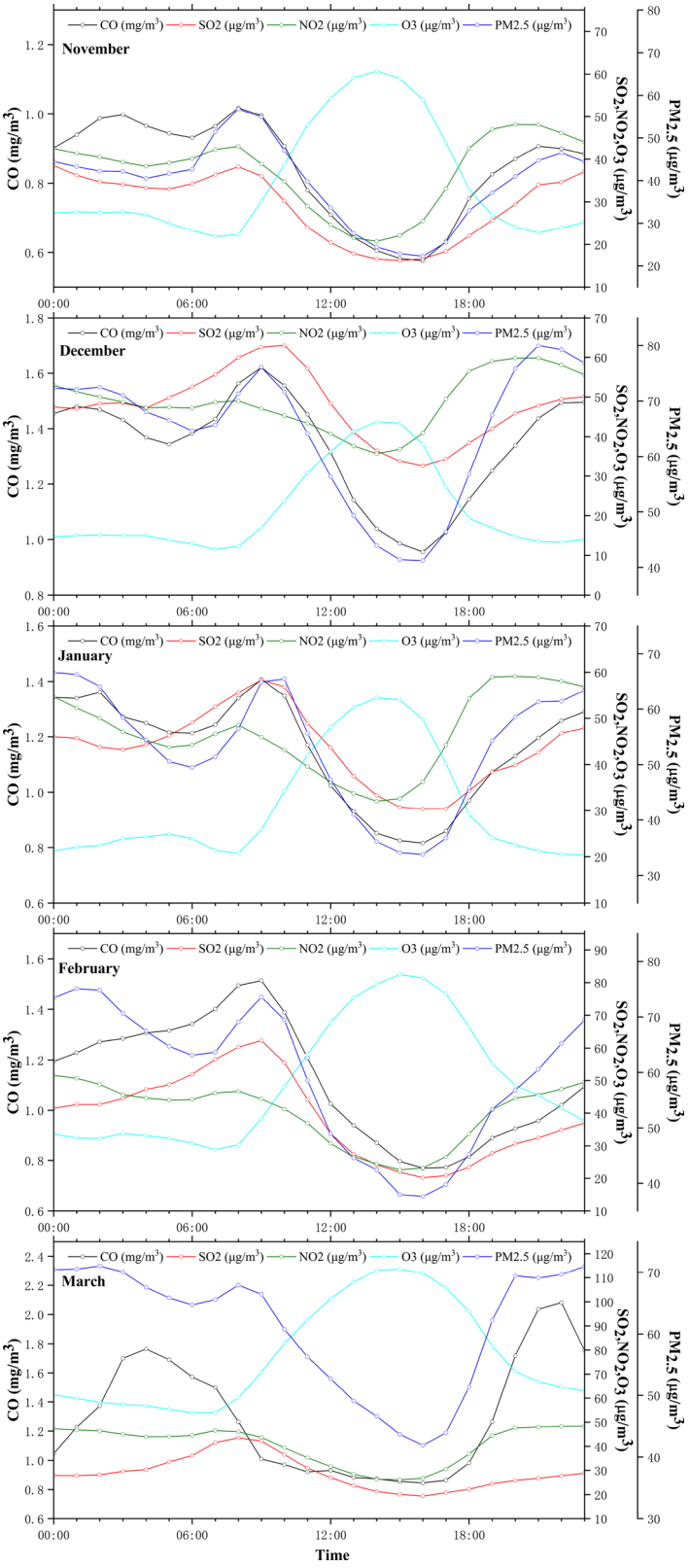

Figure 4: Diurnal variation of CO, SO_2, NO_2, O_3, and $PM_{2.5}$ concentrations in Shenyang in different months.

out in the central heating period in Shenyang, the heating coal has a certain influence on the concentration of SO_2.

Differences in daily variation of $PM_{2.5}$ in Shenyang during the five months were remarkable, and those for November were the smallest ones. It was observed that the daily variation trend for $PM_{2.5}$ concentration was similar to that of NO_2, CO, and SO_2. The peak level of $PM_{2.5}$ may indicate the burning of fossil fuels such as coal. $PM_{2.5}$ has the highest concentrations at noon in December and January. This might be related to the reduction of NO_2 and SO_2, probably indicating that the secondary formation was an important reason for the increase of $PM_{2.5}$ concentrations. The daily variation of $PM_{2.5}$ is similar to that of SO_2, demonstrating that $PM_{2.5}$ levels are related to coal combustion during the study period. $PM_{2.5}$ reached a concentration peak during the morning. Compared with NO_2 and CO, levels of $PM_{2.5}$ showed a similar increasing trend. This indicates that traffic emissions increased $PM_{2.5}$ concentrations during the morning peak hours. The $PM_{2.5}$ level began to decline, which may be due to the decrease of boundary layer height and the increase of NO_2 and CO emissions after 20:00 h. During the night, wind speeds are usually higher than during daytime, reducing the concentrations of pollutants. According to our findings, changes in boundary layer height and meteorological parameters may be the main driving factors to air pollution in the area. For future research, it is necessary to perform more measurements on the above-mentioned parameters in order to elaborate more accurate analyses.

3.3 Transmission path

The seventy-two hour backward trajectories of SLL (background) and SLXL (severe pollution) from November 1st, 2017 to March 31st, 2018 were calculated using the HYSPLIT model. Figure 5 shows the clustering trajectories (i.e., transport path) in two monitoring points. Five main backward clustering trajectories were obtained at both SLXL and SLL points. Clustering from the two points can summarize the four directions of the trajectory: south, southwest, northwest, and north. During this study, five clusters were identified for SLL: Cluster 1 – Northwest (short; NWs), Cluster 2 – Southwest (SW), Cluster 3 – North (N), Cluster 4 – Northwest (Long; NWl), and Cluster 5 – South (S). Southern air, which accounted for 12.07% of the total air mass, initiates in the southern coastal area of the Liaoning Province. In this case, the mean $PM_{2.5}$ concentration was the highest detected (64.26 μg/m^3). The southern wind carried the polluted air mass to SLL, and in 26.59% of the trajectories, $PM_{2.5}$ concentrations exceeded 75 μg/m^3. Fine particle mass concentration in the S air was heavier, with highest $PM_{2.5}/PM_{10}$ value of 0.88. The N air mass came from the Central Siberian Plateau and passed

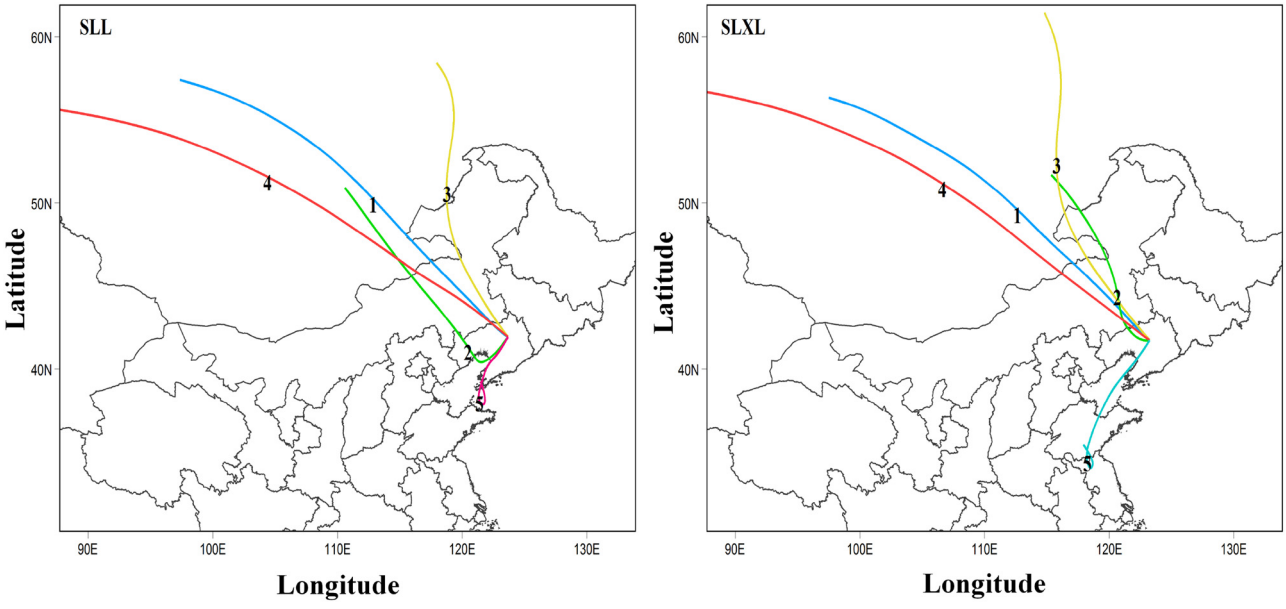

Figure 5: The back trajectory of SLL and SLXL air masses from November 2017, to March 31st, 2018.

through the Daxinganling area and the northern part of the Liaoning Province before reaching SLL. This accounted for 28.76% of the air mass. The level of air pollutants was low (mean $PM_{2.5}$ concentration was 30.46 μg/m^3), aerosol contribution to PM in SLL was also low ($PM_{2.5}/PM_{10}$, 0.60), and the air was relatively clean. NWs, SW, and NWl clusters originated from the central and western parts of Siberia and passed through eastern Mongolia and the Mongolian plateau before reaching SLL. These clusters accounted for 35.54, 15.87, and 7.77% of the air mass, respectively. These air masses were much cleaner than corresponding S air. Average $PM_{2.5}$ concentrations were 44.19, 57.2, and 43 μg/m^3, respectively. The $PM_{2.5}$ concentration of SW air mass was slightly higher than that of the other two, because SW air mass passed through the Xilingol Desert in Inner Mongolia, where there is less vegetation and bare sandy land. When the wind blows, it is easy to cause a higher concentration of particulate matter in the air above. The SW air mass may have carried additional dust and aerosols ($PM_{2.5}/PM_{10}$, 0.69). Finally, the $PM_{2.5}/PM_{10}$ ratio of the NWs and NWl air masses was higher than 0.6.

The trajectory of SLXL generated 5 clusters: cluster 1 – northwest (short; NWs), cluster 2 – north (short; Ns), cluster 3 – north (long; Nl), cluster 4 – northwest (long; NWl), and cluster 5 – South (S). Same as SLL trajectory, the S air mass of SLXL accounted for 6.78% of total air masses, and the mean $PM_{2.5}$ concentration was 73.5 μg/m^3. These air masses started in southern Shandong. The $PM_{2.5}$ concentration was greater than 75 μg/m^3 with a fraction of 37.5% in these air masses and an average $PM_{2.5}/PM_{10}$ ratio of 0.59. Nl clustering started in the Central Siberian Plateau and passed through the eastern Mongolian and Mongolian Plateaus, possibly consisting of coarse aerosols ($PM_{2.5}/PM_{10}$ value: 0.47), including 19.17% of all trajectories. However, this air was much cleaner; $PM_{2.5}$ concentration was 40.04 μg/m^3 and PM_{10} was 76.69 μg/m^3, respectively. NWs and NWl clusters demonstrated the influence of the plains of Central Siberia. In these cases, the $PM_{2.5}$ average concentrations were 61.02 and 62.51 μg/m^3, respectively. In addition, it was determined that 28.67 and 29.46% of the NWs and NWl cluster trajectories, respectively, were polluted. Moreover, SLXL was influenced by the air mass in southern Siberia (Ns air mass). The mean $PM_{2.5}$ concentration was 71.44 μg/m^3, with the $PM_{2.5}/PM_{10}$ value of 0.59, which was close to that determined for the S air mass.

By analyzing the backward trajectory of the model output, it can be found that the environmental conditions during the heating season may be affected by pollutant emissions and long-distance transportation in the region. The result is consistent with a previous study [29].

3.4 Potential source distribution

The PSCF and CWT were analyzed using the backward trajectory calculated by the model and the $PM_{2.5}$ or PM_{10} hourly monitoring concentration. This information was used to determine the potential source and contribution

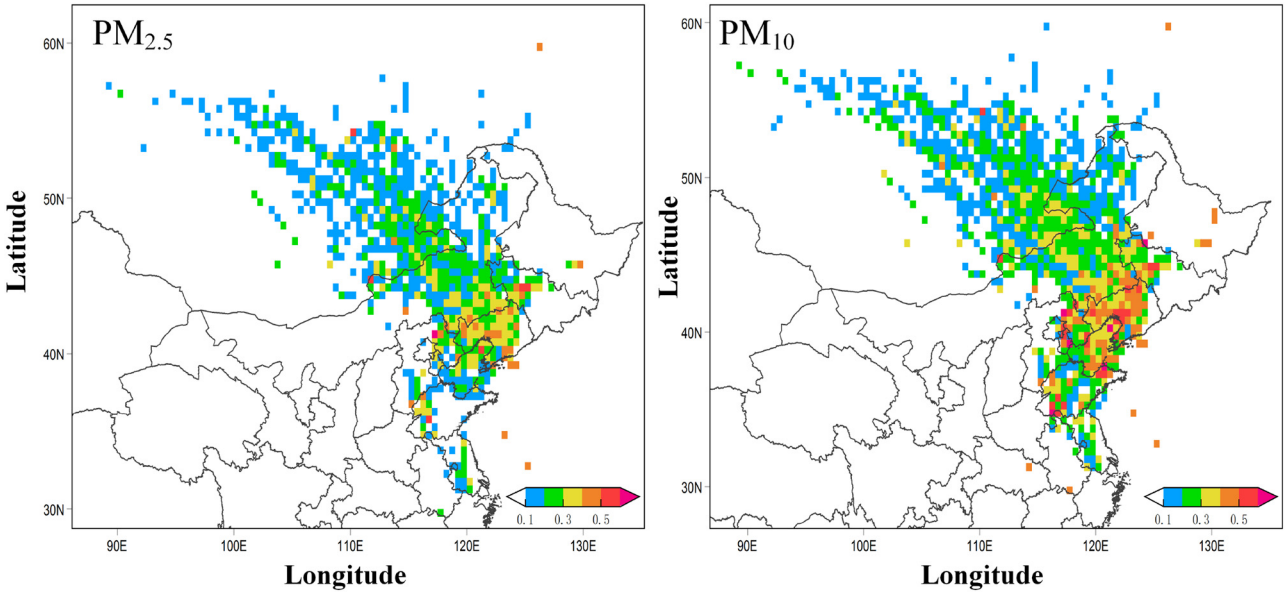

Figure 6: PSCF maps for $PM_{2.5}$ and PM_{10} in SLXL from 1 November 2017 to 31 March 2018.

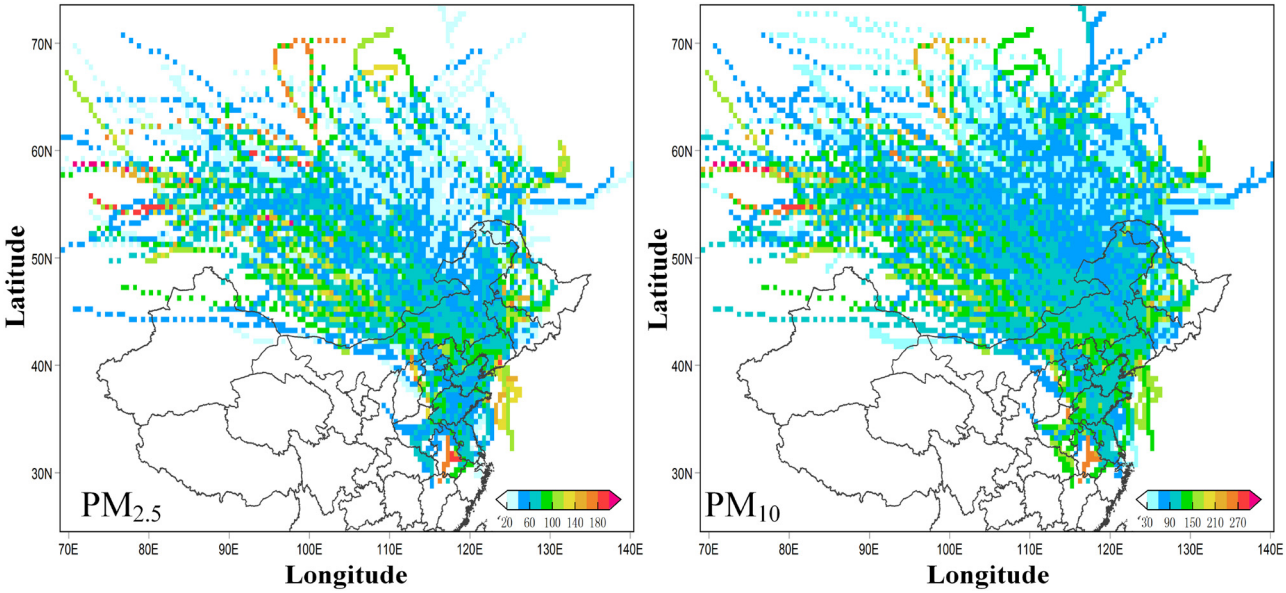

Figure 7: CWT maps for $PM_{2.5}$ and PM_{10} in SLXL from 1 November 2017 to 31 March 2018.

Table 2: Average daily concentration of $PM_{2.5}$ in eight Chinese cities including Shenyang

Cities	$PM_{2.5}$ (μg/m^3)	Location	Research period
Qingdao	85	Urban	2015/11–2016/1
Beijing	118.5	Urban/rural	2005/3–2006/2
	80.6	Urban	2012/8–2012/9
Guangzhou	108.3	Urban	2012/12–2013/2
Xi'an	194.1 (mean)	Urban	2006/3–2007/3
	288.7 (winter)		
Shanghai	83.4 (mean)	Urban	2011/12–2012/1
	104.3 (winter)		
Chengdu	206.8	Urban	2009/11–2010/1
Ji'nan	101	Urban	2013/3–2014/2
Shenyang	55	Urban	2017/11–2018/3

to the receptor site. Figures 6 and 7 show the contribution of pollution distribution in potential contaminant sources in SLXL, which was the most polluted region. Where the results of PSCF and CWT are large can be considered as potential sources of contamination in this study. PSCF in Figure 6 shows that the eastern Inner Mongolia, northwestern Jilin, and Liaoning are the main potential sources of contribution for $PM_{2.5}$ during the heating season, and the weight potential source contribution function (WPSCF) is greater than 0.3. In particular, the main source of high PM_{10} concentration is the central and western urban agglomeration of Liaoning Province. Most of the Beijing-Tianjin-Hebei area and Inner Mongolia displayed low $PM_{2.5}$ and PM_{10} contribution rates (WPSCF was less than 0.3). The Bohai Sea area in the south and the coastal cities are the potential sources for Shenyang particulate matter. (WPSCF was higher than 0.4). Overall, these findings are in accordance with findings reported by Wang et al. [35].

According to the CWT diagram in Figure 7, exogenous $PM_{2.5}$ and PM_{10} are mainly from Mongolia, Anhui, parts of the Beijing-Tianjin-Hebei region, western Jilin, and parts of Inner Mongolia. The contribution rate of $PM_{2.5}$ in the above areas is greater than 80 μg/m^3, and that of PM_{10} is greater than 120 μg/m^3. The Yellow Sea is a potential source of particulate matter in Shenyang, contributing more than 120 μg/m^3 to $PM_{2.5}$ and more than 150 μg/m^3 to PM_{10} in SLXL. As can be seen from the figure, the northwest source region has the widest distribution area and the farthest origin, which can be traced back to Mongolia and Russia. In addition, aerosols from the ocean also contributed.

3.5 Comparison with other cities

The concentrations of $PM_{2.5}$ in seven major cities in China, including Beijing [36,37], Guangzhou [38], Xi'an [33], Shanghai [39], Chengdu [40], Jinan [41], and Qingdao [42], were summarized and compared with those in Shenyang. The results are displayed in Table 2. The mean 24 h $PM_{2.5}$ concentration was widely different in varied cities, and it is related to different factors such as seasonality and detection methods. This paper analyzed

the measured data in winter, and the purpose is to better compare the $PM_{2.5}$ concentration levels in Shenyang and other cities in China. The results show that the mean $PM_{2.5}$ concentration in Shenyang was lower than other cities surveyed in the article. Among these cities, Shenyang's $PM_{2.5}$ levels are far lower than those of Beijing, Xi'an, and Chengdu. In addition, Shenyang's $PM_{2.5}$ concentration is about half that of Guangzhou and Shanghai. Also, $PM_{2.5}$ concentrations in Xi'an and Chengdu were 5.2 and 3.7 times higher than that determined in Shenyang, respectively. The annual mean $PM_{2.5}$ concentration in Jinan was 101 $\mu g/m^3$, which was 1.8 times higher than that found in Shenyang.

4 Conclusion

(1) The survey showed that the main pollutant in Shenyang in winter was $PM_{2.5}$. In 25.2% of the research days, $PM_{2.5}$ concentration during daytime was higher than the one indicated in the NAAQS limit. Among the 11 monitoring sites, SLXL usually has the highest pollution level. It is because Tiexi District is developed in heavy industrial area with many factories. It was also determined that low wind speeds and the presence of southerly or easterly winds may have contributed to the accumulation and transport of pollutants. The daily variation curve of O_3 shows a single peak shape and reaches its peak around 14:00. According to the results on daily variation of the six pollutants, coal heating and main traffic emissions are the main causes of air pollution in Shenyang.

(2) HYSPLIT model was used to calculate the back trajectories of SLL and SLXL, in order to identify the transport pathways of the pollutants. During the study period, pollutants were mainly affected by local and long-distance transport. The southern air mass mainly originated in the northern part of Jiangsu, Shandong, and the southern Liaoning Province, accounting for 6.78–12.07% of the total air mass. The average $PM_{2.5}$ concentration varied between 64.26 and 73.5 $\mu g/m^3$, and the proportion of over-standard trajectories was between 26.39 and 37.5%. The northern air mass mainly comes from Siberia, Mongolia, and other regions. The air mass from the Siberian plateau is relatively clean, diluting pollutants to some extent. The increase in particulate matter is mainly caused by increased desert aerosols from Inner Mongolia and aerosol transport from the Bohai Sea and the Yellow Sea.

(3) Use PSCF and CWT to comprehensively analyze potential sources of emissions and their contribution to PM levels. In the winter, Mongolia, eastern Inner Mongolia, northwestern Jilin, and most of Liaoning Province were the main potential source regions of $PM_{2.5}$, contributing with more than 80 $\mu g/m^3$ $PM_{2.5}$. In addition, the Beijing-Tianjin-Hebei region, the Yellow sea and Bohai sea, and Shandong and Anhui provinces also had a certain influence on the concentration of particulate matter in Shenyang. Therefore, the concentration of contaminants in Shenyang in winter may be determined by local emissions (such as coal, automobiles, anthropogenic, and industrial sources) and cross-regional transmission from surrounding areas such as Jilin, Hebei, and Inner Mongolia.

In this work, the transport path and potential sources of winter pollutants in Shenyang were deeply studied, which could provide scientific support for the joint prevention and control of regional air pollution in Shenyang and other cities. In future work, simulation of other seasons or the whole year can be added and the results of multiple monitoring stations can be selected for analysis and research. The future studies can further analyze the causes of heavy pollution weather in other seasons.

Funding information: This research was financially funded by Aeronautical Science Foundation of China (Grant No. 2017ZA54001), Industry-University Cooperation and Education Project (Grant No. 201802303005), Natural Science Foundation of Liaoning Province (No. 2021-MS-079), and National Key R&D Program of China (No. 2017YFC0212500).

Author contributions: Yunfeng Ma designed the experiments. Qiyao Liu and Yushan Bian carried them out, analyzed results, and wrote the paper. Lei Feng and Di Zhao verified the experimental results. Shuai Wang, Huijie Zhao, and Kunyu Gao prepared the experimental data. Zhengqing Xu provided software support for the experiments.

Conflict of interest: The authors declare no conflict of interest.

References

[1] Angelevska B, Atanasova V, Andreevski I. Urban air quality guidance based on measures categorization in road transport. Civ Eng J. 2021;7(2):253–67. doi: 10.28991/cej-2021-03091651.

[2] Dimitriou K. The dependence of PM size distribution from meteorology and local-regional contributions, in Valencia (Spain)-A CWT model approach. Aerosol Air Qual Res. 2015;15(5):1979–89. doi: 10.4209/aaqr.2015.03.0162.

[3] Gibergans-Baguena J, Hervada-Sala C, Jarauta-Bragulat E. The quality of urban air in Barcelona: a new approach applying compositional data analysis methods. Emerg Sci J. 2020;4(2):113–21. doi: 10.28991/esj-2020-01215.
[4] Chinese State Council. Atmospheric pollution prevention and control action plan; 2013.
[5] Ministry of Ecology and Environmental of the People's Republic of China. Report on the state of the ecology environment of china in 2017. Ministry of ecology and environmental of the People's Republic of China; 2018.
[6] China National Environmental Monitoring Centre. Air quality report of beijing-tianjin-hebei region, Yangtze river delta, pearl river delta region, municipalities directly under the central government, provincial capitals and cities listed in the plan in January 2018; 2018.
[7] Zhang Y, Cao F. Fine particulate matter ($PM_{2.5}$) in China at a city level. Sci Rep. 2015;5:14884. doi: 10.1038/srep14884.
[8] Chen XY, Li F, Zhang JD, Zhou W, Wang XY, Fu HJ. Spatiotemporal mapping and multiple driving forces identifying of $PM_{2.5}$ variation and its joint management strategies across China. J Clean Prod. 2020;250:119534. doi: 10.1016/j.jclepro.2019.119534.
[9] Wang Y, Yao L, Wang L, Liu Z, Ji D, Tang G, et al. Mechanism for the formation of the January 2013 heavy haze pollution episode over central and eastern China. Sci China Earth Sci. 2014;57(1):14–25. doi: 10.1007/s11430-013-4773-4.
[10] Chen Y, Ebenstein A, Greenstone M, Li H. Evidence on the impact of sustained exposure to air pollution on life expectancy from China's Huai River policy. Proc Natl Acad Sci. 2013;110(32):12936–41. doi: 10.1073/pnas.1300018110.
[11] Zhang R, Jing J, Tao J, Hsu SC, Wang G, Cao J, et al. Chemical characterization and source apportionment of $PM_{2.5}$ in Beijing: seasonal perspective. Atmos Chem Phys. 2013;13(14):7053–74. doi: 10.5194/acp-13-7053-2013.
[12] General Office of Shenyang Municipal Government. Notice of the general office of shenyang municipal people's government on printing and distributing the plan of total coal consumption control in shenyang in 2016; 2016.
[13] Shenyang Municipal Bureau of Statistics. Shenyang statistical yearbook; 2018.
[14] Zhao H, Che H, Zhang X, Ma Y, Wang Y, Wang H, et al. Characteristics of visibility and particulate matter (PM) in an urban area of Northeast China. Atmos Pollut Res. 2013;4(4):427–34. doi: 10.5094/APR.2013.049.
[15] Zhang J, Liu L, Wang Y, Ren Y, Wang X, Shi Z, et al. Chemical composition, source, and process of urban aerosols during winter haze formation in Northeast China. Environ Pollut. 2017;231(5):357–66. doi: 10.1016/j.envpol.2017.07.102.
[16] Miao Y, Guo J, Liu S, Zhao C, Li X, Zhang G, et al. Impacts of synoptic condition and planetary boundary layer structure on the trans-boundary aerosol transport from Beijing-Tianjin-Hebei region to northeast China. Atmos Environ. 2018;181:1–11. doi: 10.1016/j.atmosenv.2018.03.005.
[17] Zong Z, Wang X, Tian C, Chen Y, Fu S, Qu L, et al. PMF and PSCF based source apportionment of $PM_{2.5}$ at a regional background site in North China. Atmos Res. 2018;203:207–15. doi: 10.1016/j.atmosres.2017.12.013.
[18] Yang L, Chen CL, Cao ST, Sun L, Cui YP, Jiang C, et al. Comprehensive analysis of a heavy $PM_{2.5}$ pollution event over Shenyang in November of 2015. J Meteorol Environ. 2019;35(3):37–44. doi: 10.3969/j.issn.1673-503X.2019.03.005.
[19] Ma YJ, Li XL, Zhang YH, Hong Y, Zhao HJ, Wang YF, et al. Analysis of the mechanism of a heavy pollution in December 2016 at Shenyang. Environ Chem. 2020;39(12):3346–52. doi: 10.7524/j.issn.0254-6108.2019091204.
[20] Duan YX, Li DQ, Tian L, Wang SD, Sun X, Wu YT, et al. Characteristic analysis of a continuous and serious pollution weather process in shenyang. J Arid Meteorol. 2016;34(5):803–10. doi: 10.11755/j.issn.1006-7639(2016)-05-0803.
[21] Draxler R, Hess G. An overview of the HYSPLIT_4 modelling system for trajectories. Aust Meteorol Mag. 1998;47:295–308.
[22] Draxler R, Stunder B, Rolph G, Stein A, Taylor A. HYSPLIT4 user's guide. Air resources laboratory, National Oceanic and Atmospheric Administration (NOAA). Silver Spring, MD; 2014.
[23] Wang YQ, Zhang XY, Draxler RR. TrajStat: GIS-based software that uses various trajectory statistical analysis methods to identify potential sources from long-term air pollution measurement data. Environ Model & Softw. 2009;24(8):938–9. doi: 10.1016/j.envsoft.2009.01.004.
[24] Kim IS, Lee JY, Wee D, Kim YP. Estimation of the contribution of biomass fuel burning activities in North Korea to the air quality in Seoul, South Korea: Application of the 3D-PSCF method. Atmos Res. 2019;230:104628. doi: 10.1016/j.atmosres.2019.104628.
[25] Ashbaugh LL, Malm WC, Sadeh WZ. A residence time probability analysis of sulfur concentrations at grand Canyon national park. Atmos Environ (1967). 1985;19(8):1263–70. doi: 10.1016/0004-6981(85)90256-2.
[26] Li D, Liu J, Zhang J, Gui H, Du P, Yu T, et al. Identification of long-range transport pathways and potential sources of $PM_{2.5}$ and PM_{10} in Beijing from 2014 to 2015. J Environ Sci. 2017;56:214–29. doi: 10.1016/j.jes.2016.06.035.
[27] Mukherjee A, Agrawal M. Assessment of local and distant sources of urban $PM_{2.5}$ in middle Indo-Gangetic plain of India using statistical modeling. Atmos Res. 2018;213:275–87. doi: 10.1016/j.atmosres.2018.06.014.
[28] Zhang H, Cheng S, Wang X, Yao S, Zhu F. Continuous monitoring, compositions analysis and the implication of regional transport for submicron and fine aerosols in Beijing, China. Atmos Environ. 2018;195:30–45. doi: 10.1016/j.atmosenv.2018.09.043.
[29] Tian JQ, Fang CS, Qiu JX, Wang J. Analysis of pollution characteristics and influencing factors of main pollutants in the atmosphere of Shenyang city. Atmosphere. 2020;11(7):766. doi: 10.3390/atmos11070766.
[30] Zhang Y, Zhu X, Slanina S, Shao M, Zeng L, Hu M, et al. Aerosol pollution in some Chinese cities (IUPAC Technical Report). Pure Appl Chem. 2004;76(6):1227–39. doi: 10.1351/pac200476061227.
[31] Bergin MH, Cass GR, Xu J, Fang C, Zeng LM, Yu T, et al. Aerosol radiative, physical, and chemical properties in Beijing during June 1999. J Geophys Research: Atmospheres. 2001;106(D16):17969–80. doi: 10.1029/2001JD900073.
[32] Guo S, Hu M, Zamora ML, Peng J, Shang D, Zheng J, et al. Elucidating severe urban haze formation in China. Proc Natl Acad Sci. 2014;111(49):17373–8. doi: 10.1073/pnas.1419604111.
[33] Zhang T, Cao J, Tie X, Shen Z, Liu SX, Ding H, et al. Water-soluble ions in atmospheric aerosols measured in Xi'an,

China: Seasonal variations and sources. Atmos Res. 2011;102:110–9. doi: 10.1016/j.atmosres.2011.06.014.
[34] Shao M, Zhang Y, Zeng L, Tang X, Zhang J, Zhong L, et al. Ground-level ozone in the Pearl River Delta and the roles of VOC and NOx in its production. J Environ Manag. 2009;90(1):512–8. doi: 10.1016/j.jenvman.2007.12.008.
[35] Wang S, Lin H, Wang JN, Shao CY, Liu M, Ma YF, et al. Analysis of the transport path and potential source of air particles in Shenyang during the winter. Environ Prot Sci. 2021;47(1):80–6. doi: 10.16803/j.cnki.issn.1004-6216.2021.01.013.
[36] Yang F, Tan J, Zhao Q, Du Z, He K, Ma Y, et al. Characteristics of PM $_{2.5}$ speciation in representative megacities and across China. Atmos Chem Phys. 2011;11(11):5207–19. doi: 10.5194/acp-11-5207-2011.
[37] Zhang Y, Huang W, Cai T, Fang D, Wang Y, Song J, et al. Concentrations and chemical compositions of fine particles ($PM_{2.5}$) during haze and non-haze days in Beijing. Atmos Res. 2016;174:62–9. doi: 10.1016/j.atmosres.2016.02.003.
[38] Wang J, Ho SSH, Ma S, Cao J, Dai W, Liu S, et al. Characterization of $PM_{2.5}$ in Guangzhou, China: Uses of organic markers for supporting source apportionment. Sci Total Environ. 2016;550:961–71. doi: 10.1016/j.scitotenv.2016.01.138.
[39] Wang F, Guo Z, Lin T, Rose N. Seasonal variation of carbonaceous pollutants in $PM_{2.5}$ at an urban 'supersite' in Shanghai, China. Chemosphere. 2016;146:238–44. doi: 10.1016/j.chemosphere.2015.12.036.
[40] Tao J, Zhang L, Engling G, Zhang R, Yang Y, Cao J, et al. Chemical composition of $PM_{2.5}$ in an urban environment in Chengdu, China: importance of springtime dust storms and biomass burning. Atmos Res. 2013;122:270–83. doi: 10.1016/j.atmosres.2012.11.004.
[41] Wang Y, Hu J, Zhang H, Ying Q. Spatial and temporal variability of $PM_{2.5}$ and PM_{10} over the North China Plain and the Yangtze River Delta, China. Atmos Environ. 2014;95:598–609. doi: 10.1016/j.atmosenv.2014.07.019.
[42] Li L, Yan D, Xu S, Huang M, Wang X, Xie S. Characteristics and source distribution of air pollution in winter in Qingdao, Eastern China. Environ Pollut. 2017;224:44–53. doi: 10.1016/j.envpol.2016.12.037.